11th EAWE PhD Seminar on Wind Energy in Europe
23-25 September 2015
Stuttgart, Germany
Session XXXX Paper XXXXXXX

Steady and unsteady CFD power curve simulations of generic 10 MW turbines

Eva Jost[1], Thorsten Lutz, Ewald Krämer
Institute of Aerodynamics and Gas Dynamics, University of Stuttgart
Pfaffenwaldring 21, 70569 Stuttgart, Germany
[1]e.jost@iag.uni-stuttgart.de

Keywords – Aerodynamics, CFD simulation, AVATAR reference wind turbine, DTU 10 MW reference wind turbine, power curve

The present study investigates the aerodynamics of large wind turbines by means of CFD. Two generic turbines of 10 MW size, the DTU 10 MW rotor [1] and the AVATAR rotor [2], have been simulated with the code FLOWer [3]. The focus was put on the comparison between unsteady and steady simulations. Unsteady results showed that large-scaled flow separation is occurring at the blade root leading to pressure fluctuations on the surface. Especially in above-rated conditions an influence on integral power and thrust is observed.

I. Introduction

One of the main focus points of today's wind energy research is the development of large Multi-Mega-Watt turbines of 10 MW to 20 MW size. This trend is driven by the ambition to reduce the overall cost of energy, which can be achieved by increasing the power output per turbine at moderate rise of manufacturing costs. Raising the rotor diameter is one promising way for attaining this goal.

However, the development of these novel turbines is connected to severe technical challenges. As simple up-scaling will lead to heavy-weight rotors, new design philosophies have to be applied to reduce mass and loads. For the DTU 10 MW [1] and AVATAR [2] reference wind turbines the rotor weight was reduced by selecting thicker airfoils to increase the moment of inertia and therefore blade stiffness. Large rotors are also distinguished by changed aerodynamic characteristics compared to current market turbines. The increased diameter leads to a higher Reynolds number regime on the airfoils. Due to the increased tip speed, the occurrence of compressibility at the blade tip is possible.

Detailed investigations are necessary to evaluate and analyse these effects. Within this study the AVATAR and DTU 10 MW reference wind turbine are examined by means of compressible CFD. Different operating conditions were investigated in a 120 degree model with periodic boundary conditions. In terms of validation the results have been compared with the partners of the European FP7 project AVATAR [3].

II. Reference Wind Turbines

In Table 1 the major characteristics of both turbines are listed and opposed to each other. The DTU 10 MW turbine is a generic offshore turbine [1]. Its rotor radius is 89.15m and as baseline airfoil family the FFA-W3-xxx group was chosen. At the inner blade region, a rigid Gurney flap is applied to achieve a higher aerodynamic performance.

Turbine	**DTU 10 MW** [1]	**AVATAR** [2]
Rated power	10 MW	10 MW
Rated wind speed	11.4 m/s	10.5 m/s
Rotor diameter	178.3 m	205.8 m
Hub height	119 m	132.7 m
Operating range	4 – 25 m/s	
Max. RPM	9.6	9.6
Optimal power coefficient	0.4776	0.438

Table 1: Reference wind turbine characteristics

The AVATAR rotor has a greater radius of 102.88m and consists of different DU profiles. In terms of load reduction and wind farm aspects it is designed as low induction blade [2].

III. Simulation Process Chain

For the present work, the process chain for the simulation of wind turbines of the Institute of Aerodynamics and Gas Dynamics (IAG), University of Stuttgart [4], was used. The main part constitutes the CFD code FLOWer, which was developed by the German Aerospace Center (DLR) [5] and enhanced at the IAG with extension for the simulation of wind turbines.

FLOWer is a compressible code that solves the three dimensional, Reynolds averaged Navier Stokes equations in integral form. The numerical scheme is based on a finite volume formulation for block-structured grids. To determine the convective fluxes, a second order central discretisation with artificial damping is used, also called the Jameson-Schmidt-Turkel (JST) method. The time integration is accomplished by an explicit multi-stage scheme including local time-stepping. Time accurate simulations make use of the Dual-time-stepping method as an implicit scheme. To close the Navier Stokes equation system, several state of the art turbulence models can be applied, as for example the model by Menter [6], which is used for this study. There are two main code features for the simulation of wind turbines. The ROT module for moving and rotating reference frames in combination with the CHIMERA technique [7] for overlapping meshes allow body motions relative to each other.

The generation of the blade grid is automated with a script for the grid generator Gridgen by Pointwise®. Blade grids are of C-type with a tip block and coning towards the blade root. For a pure rotor simulation as used in this study, the blade grid is placed in 120 degree background grid with periodic boundary conditions. Figure 1 shows the DTU 10 MW rotor setup including spinner and nacelle.

On the post-processing side, loads are determined through the integration of the pressure and friction distribution over the blade surface. Spanwise distributions of the forces are generated similarly dividing the blade into different sections.

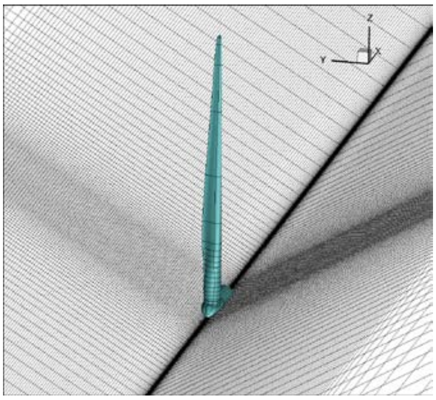

Figure 1: 120 degree turbine model

IV. Computational Setup

The simulation mesh consists of four separate grids for background, nacelle, spinner and blade, which are overlapped using the CHIMERA technique. As the geometry of spinner and nacelle is identical for both turbines, the same grids were used. The nacelle grid is of cylindrical shape and consists of approximately 1.5 million cells. Around 1.4 million cells were used for the spinner grid including blade connection.

The resolution of the different blade grids is listed in the following Table 2. For the DTU 10 MW turbine a higher amount of nodes had to be used around the airfoil in order to accurately mesh the Gurney flap at the blade root. Hence, the total amount of grid cells is slightly higher.

	DTU 10 MW	AVATAR
Chordwise nodes	221	201
Spanwise nodes	131	141
Total amount of grid cells	6.84e6	6.62e6

Table 2: Blade grid resolutions

Caused by the different blade radii, two background grids had to be generated. For the AVATAR rotor the refinement at rotor location had to be extended further outboard due to the larger radius. This leads to a higher amount of grid cells. The AVATAR background grid consists of approximately 5.9 million cells, while the DTU 10 MW background grid has a size of 5.6 million cells. In both cases the discretisation around the rotor is about 1m.

In summary, a total of 15.42 millions cells had to be used for the AVATAR turbine and respectively 15.34 millions for the DTU 10 MW turbine.

V. Validation Results

A. Grid convergence study

At first the results for the DTU 10 MW turbine will be shown. Three different resolutions were investigated within the grid convergence study and the amount of grid cells varies from 7.45 to 30.25 million. All simulations were performed unsteady with a time step corresponding to 2° blade azimuth and 100 inner iterations. The results have been averaged over one resolution. Figure 1Figure 2 shows spanwise distributions of torque and thrust. A good accordance between the fine and medium grid can be seen. Thrust is well aligned for all three grids while torque shows a larger discrepancy to the coarse grid. The reason is that thrust is a pressure driven force while in the driving component a big influence of frictional parts is apparent. To resolve the frictional effects correctly an adequate resolution is needed and hence the resolution of the coarse grid is not high enough.

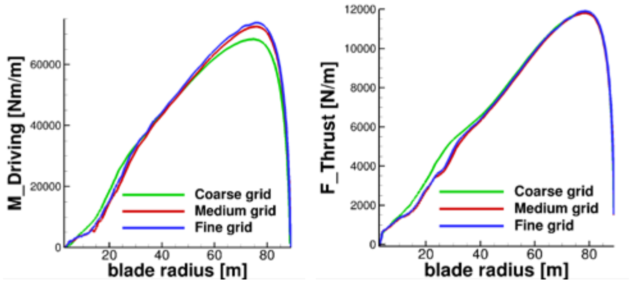

Figure 2: Grid convergence DTU 10 MW turbine

For the AVATAR turbine, the grid convergence study shows similar findings as for the DTU 10 MW turbine. A good accordance between fine and medium grid is seen in Figure 3 and the spread between the different grids is higher in torque than in thrust.

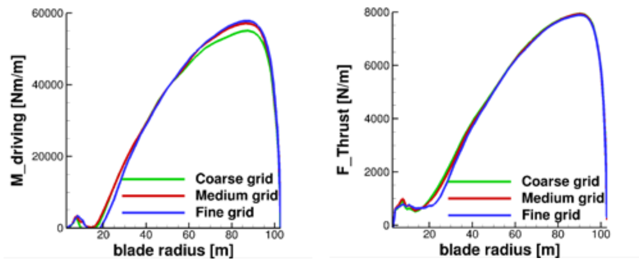

Figure 3: Grid convergence AVATAR turbine

B. Integral power curve

Measurement results of 10 MW turbines are not available for now and the nearer future. Therefore, it is necessary to compare different codes to each other to judge validity of the computations und achieve sufficient reliability. Within the AVATAR project [3], the results of this study have been compared to those of partners. The following chapter presents some of the results in terms of validation.

Different codes of different complexity were included into the study. For reasons of clarity in the diagrams only the CFD codes will be shown here and in case of the DTU 10 MW turbine only the partners, who simulated the full wind speed range. Apart from EllipSys3D of Risø DTU, all included codes are compressible solvers. All simulations were performed steady state with a stiff blade.

In Figure 4, a comparison of the power curve is shown. A good accordance between the different codes EllispSys3D, MaPFlow and FLOWer can be observed. Only in the above-rated cases minor differences appear. The development of thrust versus wind speed is shown in Figure 5. Again the curves agree well in below-rated conditions while at higher wind speeds a slight discrepancy can be observed.

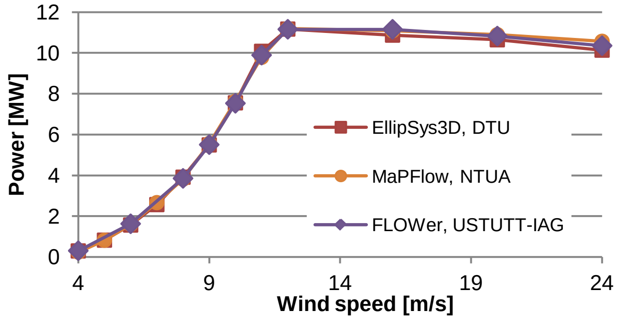

Figure 4: DTU 10 MW power curve (modified from [3])

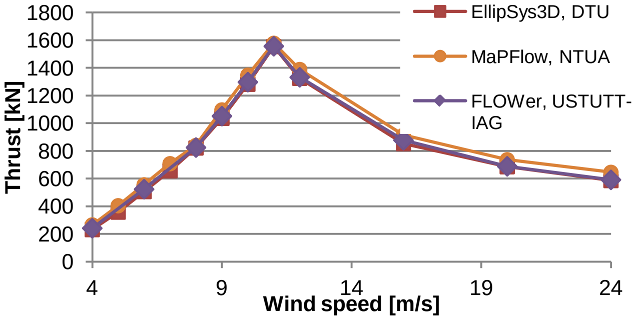

Figure 5: DTU 10 MW thrust curve (modified from [3])

For the AVATAR turbine only the below-rated regime was investigated and is shown in Figure 6 and Figure 7. While thrust agrees well in most cases, a larger spread in power is observed. The code by CENER and ULIV predicts a higher power output than EllipSys3D, MaPFlow and FLOWer.

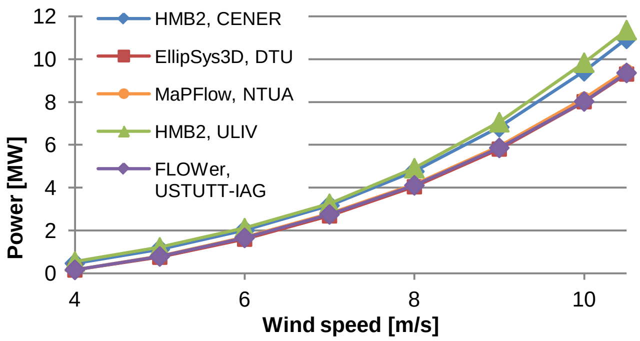

Figure 6: AVATAR power curve (modified from [3])

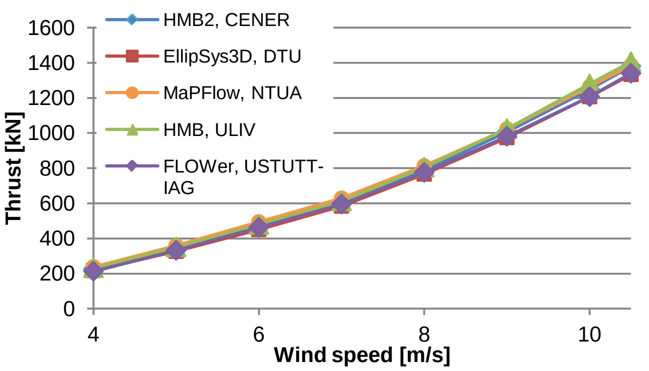

Figure 7: AVATAR thrust curve (modified from [3])

Nevertheless, the setup under investigation showed plausible results and can therefore be regarded as suitable for further examinations und studies.

VI. Steady vs. Unsteady Simulations

The next step was to analyse the influence of unsteady effects on the turbine loads. Especially at the root where the blade is of cylindrical shape, a strong influence of flow separation and vortex shedding is expected. To judge these effects, the simulations were repeated in unsteady mode with a time step corresponding to 2° blade azimuth. Only the results of the DTU 10 MW turbine are presented here. Two different wind speeds, 12 m/s and 20 m/s, have been investigated. The results of the steady simulations are compared to those of the averaged unsteady simulations. In Figure 8, sectional force distributions of torque are plotted versus blade radius for the different computations. Figure 9 shows the respective diagram for thrust.

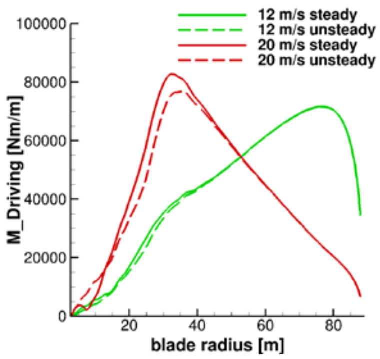

Figure 8: Torque – comparison steady/unsteady

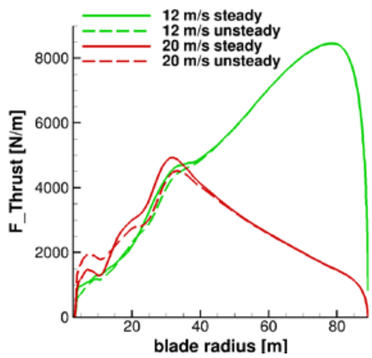

Figure 9: Thrust– comparison steady/unsteady

At the outer blade part, starting from approximately 45 percent of the blade radius, the curves are mostly identical in both diagrams and therefore the influence of unsteady effects can be neglected there. As expected, differences between the two computations appear at the blade root.

To get further insight pressure distributions were extracted. Figure 10 shows extractions for 12 m/s wind speed at the blade stations with radius 16m and 22m.

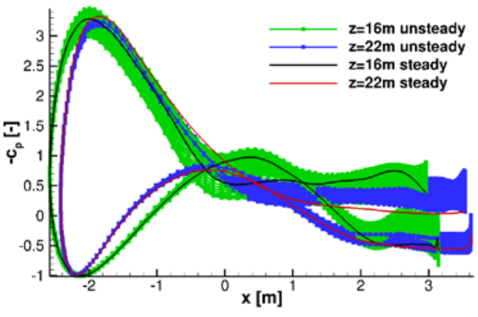

Figure 10: cp distributions – blade root, 12 m/s

At both cuts the steady and unsteady solutions show major differences in mean values and strong fluctuations appear at the rearward part. Figure 11 displays the same extractions at 20 m/s wind speed, in which higher variation is seen in the results. Caused by earlier flow separation the unsteady effects have increased.

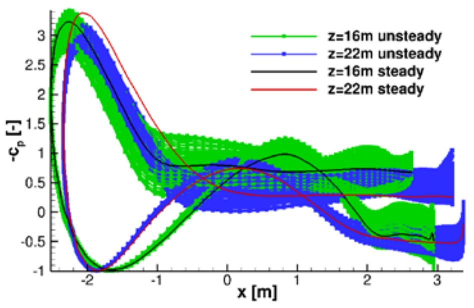

Figure 11: cp distributions – blade root, 20 m/s

In the unsteady simulation at 12 m/s the averaged integral power is 10.97 MW compared to 11.16 MW in steady mode. Thrust is in both cases nearly identical with 1330 kN and 1313 kN respectively. At 20 m/s the power decreased from 10.83 MW to 10.34 MW and thrust reduced from 705 kN to 672 kN. In summary it can be stated that for the determination of integral values such as power and thrust the effects of the root separation is dependent on the regarded wind speed. At higher wind speeds in above-rated cases inner blade regions become more important and additionally unsteady phenomena increase. For these cases variations of 5 percent have been observed and therefore the steady computation can only serve as first estimation. To some extent this can also explain the larger differences observed at higher wind speeds in the power curve validation.

VII. CONCLUSION

Within the present work the power curve of two generic 10 MW wind turbines was examined by means of CFD. Steady and unsteady simulations have been performed. The steady simulations were validated against the results of partners in the AVATAR project. A good accordance with the codes EllipSys3D and MaPFlow is observed. The unsteady simulations showed large scaled flow separation at the blade root leading to pressure fluctuations on the surface. It was found that these effects have a great influence on the sectional loads in this blade area. The importance for the determination of the integral characteristics is dependant on the wind speed. At above-rated conditions unsteady effects increase and inner blade parts become more important for the turbine power and loading. Unsteady simulations become necessary for accurate predictions.

ACKNOWLEDGEMENTS

For providing their resources the authors gratefully thank the High Performance Computing Center Stuttgart and the European FP7 project AVATAR for funding.

REFERENCES

[1] C. Bak, F. Zahle, R. Bitsche, T. Kim, A. Yde, L. Henriksen, P. Andersen, A. Natarajan and M. Hansen, “Design and performance of a 10 MW turbine,” *J. Wind Energy*, To be accepted.

[2] G. Sieros, D. Lekou, D. Chortis, P. Chaviarapoulos, X. Munduate, A. Irisarri, H. A. Madsen, K. Yde, K. Thomsen, M. Stettner, M. Reijerkerk, F. Grasso, R. Savenije, G. Schepers and C. Andersen, “AVATAR Deliverable D1.2 - Reference Blade Design,” 2015.

[3] N. Sørensen, M. Hansen, N. Garcia, L. Florentie, K. Boorsma, S. Gomez-Iradi, J. Prospathopoulus, G. Barakos, Y. Wang, E. Jost and T. Lutz, “AVATAR Deliverable 2.3: Power Curve Predictions,” 1 June 2015. [Online]. Available:http://www.eera-avatar.eu/fileadmin/mexnext/user/report-d2p3.pdf.

[4] K. Meister, E. Krämer and T. Lutz, “Development of a process chain for detailed wake simulation of horizontal axis wind turbines,” in *EUROMECH*, Madrid, 2009.

[5] N. Kroll and J. Fassbender, MEGAFLOW – Numerical Flow Simulation for Aircraft Design, Berlin/Heidelberg/New York: Springer Verlag, 2002.

[6] F. Menter, “Two-Equation Eddy-Viscosity Turbulence Models for Engineering Applications,” *AIAA Journal*, vol. 32, pp. 1598-1605, 1994.

[7] J. Benek, J. Steger, F. Dougherty and P. Buni, “Chimera: A Grid-Embedding Technique,” Arnold Engineering Development Center; Arnold AFS TN.;, 1986.